

MODELING SOLAR CELLS: A METHOD FOR ACHIEVING IMPROVED EFFICIENCIES

**Arturo Morales-Acevedo, Norberto Hernández-Como and
Gaspar Casados-Cruz**

Centro de Investigación y de Estudios Avanzados del IPN
Electrical Engineering Department
Avenida IPN No. 2508, 07360 Mexico, D. F. (Mexico)
amorales@solar.cinvestav.mx

1. Introduction

Numerical simulation is now almost indispensable for the understanding and design of solar cells based on crystalline, polycrystalline and amorphous materials. Highly developed programs include effects due to tunneling, optical light trapping, heat flow and other features. In principle, any numerical program capable of solving the basic semiconductor equations could be used for modeling conventional homo-junction and thin-film solar cells. These basic equations are the Poisson equation and the continuity equations for electrons and holes. In general, the recombination terms, contained in the continuity equations, make the problem highly non-linear, but numerical methods for dealing with such equations has been already developed.

Our basic approach for developing and designing improved solar cells has been to have a basic understanding of the specific solar cell physical behavior by means of simple analytical models first and then proceed to make detailed and more exact calculations with the help of simulation programs. When this approach has been used, having to simulate many cases has been avoided, except for those with the greatest physical significance, in such a way that the results can be understood in a more complete manner than doing simulations without any previous knowledge. Sometimes, the numerical simulations provide new features, in addition to more exact calculations, as compared to the analytical model calculations. Proceeding in this way, the importance of numerical calculations is revealed in a more precise way. In other words, in a similar manner to real experiments, the simulation of solar cells has to be planned based on previous analytical model results that involve the basic physics of solar cells. Optimization of these devices can then be realized in a more straightforward manner, as will be shown by some examples below. This approach has been more useful when applied to the new thin film solar cells

In this paper, as an example of the above approach, we will describe and explain the numerical simulation results for two different solar cell structures, pointing out the importance of the new features provided by the simulation results. The first case refers to HIT solar cells on silicon. It will be shown that numerical simulation allows us to define the best TCO layer regarding the work function, in addition to the required low interface state density at the silicon surface. The second case refers to CdS/CIGS solar cells. It will be shown that this kind of solar cells is complex, and not completely understood, so that many electrical parameters are not well known, making it difficult to generate an appropriate model. In addition, it will be shown that the real structure has not been determined experimentally, particularly for those cells reported with efficiencies above 18%, which is the maximum efficiency obtained numerically for a simple CdS/CIGS solar cell. Explaining the laboratory efficiencies above 20% can not be done with present (numerical) models and then it will be necessary to make further experiments to obtain information about the material properties and the real structure for this kind of solar cells in order to have a more realistic model. In this case, the interaction between modeling and experimental results can be used for guiding us in defining the required experiments.

2. Solar cell simulation tools

Before proceeding to the above discussion we shall make a short review of some of the freely distributed simulation tools. These programs are mostly reduced to one dimensional analysis as compared with highly expensive commercial programs which can make two and three dimensional device simulations and requiring workstations for running.

2.1. PC1D

This program was developed by Basore and coworkers originally at Sandia National Labs and was further developed at UNSW, Australia (Basore, 1990; Clugston and Basore, 1997). It is considered a standard for crystalline Si cells, and it is widely spread in the PV research community, and hence also used for some thin-film cells, though it is not particularly designed for those cells. Being originally developed for crystalline silicon cells the number of layers is rather limited, only five layers are allowed per device. For CdTe/CdS-based devices this is probably enough provided that the doping of the layers is not graded, but for CIGS based devices this number is low. All of the most common recombination mechanisms are implemented: Auger, band-to-band and trap-assisted tunneling (Hurkx et al., 1992). It is not possible to define a general Density of States (DOS) distribution; only one deep level can be specified per layer by giving its position in the forbidden gap and the lifetimes for electrons and holes. Because no densities of deep levels can be given, there is no space charge connected with these levels. This is a problem when modeling II-VI and a-Si solar cells, where the charge contained in deep states can play an essential role. Besides the standard $J(V)$ and spectral response measurements, transients can also be simulated. Light or bias voltage can suddenly be applied and the effect on the device can be monitored as a function of time.

2.2. SCAPS-1D

SCAPS (a Solar Cell Capacitance Simulator) is a numerical simulation program written and maintained at the University of Gent (Burgelman et al., 2000). It is designed as a general polycrystalline thin-film device simulator and is mainly used for modeling CdTe- and CIGS/CIS-based solar cells. Up to seven layers can be added to the device and for each layer or contact all physical and electronic properties can be shown and altered inside a separate window. Simple models are used for the temperature dependence of the effective density of states and the thermal velocity, other parameters such as the band-gap and the mobilities are independent of temperature. For each layer, up to three deep levels can be defined, and in between two layers up to three interface states can be placed. These deep levels can be energetically distributed in the band-gap (single level, uniform, gauss or exponential tail). The deep bulk levels can also vary spatially inside the layer (uniform, step, linear or exponentially). All other properties can be graded for each layer in the device. Recombination in deep bulk levels and their occupation is described by the Shockley–Read–Hall (SRH) formalism. Recombination at the interface states is described by an extension of the SRH formalism (Pauwels and Vanhoute, 1978), allowing the exchange of electrons between the interface states and the two adjacent conduction bands, and of holes between the states and the two adjacent valence bands. SCAPS has among the studied simulation programs the largest number of electrical measurements that can be simulated: $J(V)$, $C(V)$, $C(f)$ and spectral response. Each measurement can be calculated for light or dark conditions and as a function of temperature. When solving the desired simulations, the energy band diagram and the charge and currents in the device are shown on screen for each intermediate bias voltage or wavelength.

2.3. AMPS-1D

AMPS (Analysis of Microelectronic and Photonic Structures) was written by S. Fonash and coworkers of Pennsylvania State University (www.ampsmodeling.org, August 2011). It is a very general and versatile computer simulation tool for the analysis of device physics and for device design. A single device can have up to 30 layers, each layer having its own set of parameters. All parameters (bandgap, effective density of states, mobilities) are independent of temperature. For each layer a total of 50 deep donor and acceptor levels can be assigned, resulting in the possibility of creating an almost arbitrary density of states distribution. The deep levels can be energetically distributed in the band-gap (discrete, uniform or gaussian). In addition, it is possible to define exponential band tail states. All properties of a layer are spatially uniform. By adding different layers with gradually changing parameters, however, it is possible to simulate graded junctions. AMPS can handle up to 3000 nodes, but direct tunneling, amphoteric and interface states are not included. When the definition of the device is completed, the user can choose to simulate $J(V)$ in both light and dark conditions as well as spectral response measurements. AMPS is slow in solving the problem when compared with other simulation programs. The ability to solve several cases simultaneously, combined with a remarkable stability, makes this program suitable to use in a batch mode. Once the results are calculated, they can be analyzed with the built-in plotting facility. One of the major drawbacks in this program is the

absence of trap states at the interface between two layers. However, this can be solved by means of a “trick”, i.e. by having a very thin region with a high (bulk) band-gap distribution of states between the two regions. We have used this trick in order to simulate HIT silicon solar cells (Hernandez-Como and Morales-Acevedo, 2010) with AMPS, as will be explained below.

2.4. Other Programs

Many other numerical simulation programs than those discussed here are in use. SimWindows (www.simwindows.com, August 2011) is a freely available one-dimensional drift/diffusion simulator for semiconductor devices. It can handle tunneling and incorporates internal heat generation in its calculations. ADEPT-F from the group of Jeff Gray, Purdue University (Gray, 1991) has been widely used. A version for the Windows operating system is to be issued shortly. The program ASPIN of the University of Ljubljana (Smole et al., 1994) has been used for CIGS cells and for a-Si cells. AFORS-HET has been developed by a group of the Hahn-Meitner Institute of Berlin (Froitzheim et al., 2003). Programs such as SILVACO-ATLAS and CrossLight-APSYS are expensive commercial programs used in silicon microelectronic industry; though in principle they are also usable for solar cells, they are specially developed for microelectronic devices, and some also implement simulation of Si wafer processing. They often offer true multi-dimensional (two- or three-dimensional) simulation. Polycrystalline thin-film solar cells properly require the use of two- or even three-dimensional programs because of grain boundaries and non-planar interfaces. Grain boundary effects seem to be more prominent in CdTe cells than in CIGS cells. Though one-dimensional problems effectively average the effect of grain boundary states over the bulk, they have been surprisingly successful. Also, transition to two or three dimensions will increase substantially the number of input parameters, many of which are presently not well known.

3. The relevance of solar cell numerical modeling

We already have explained that numerical simulation would help whenever there is a previous analysis of the solar cells to be studied by means of analytical models. Before any solar cell simulation problem is attempted a good understanding of the cell structure and the physical parameters involved is required. This sometimes is not possible because there is not a full characterization of the real cell structure. For example, the real structure for CdS/CIGS solar cells is not well known because an interfacial layer between the CdS and the CIGS layer may appear with special properties depending upon the cell preparation method. It has been suggested that close to this interface a thin inversion (n-type) CIGS layer exist in contact with a more stoichiometric p-type CIGS layer. The presence and properties of this layer will depend upon the deposition method and conditions for both the CIGS and the CdS layers. Sometimes, some parameters which are well known for bulk materials are not adequately known for thin polycrystalline materials, and therefore it is not easy to select the appropriate values for simulating the solar cells based on such materials. In addition, experimental groups usually report the efficiency of solar cells, but not the properties of each of the layers and viceversa. Therefore, there will be some uncertainty on the real values for the physical parameters such as electron affinity, carrier mobility and lifetime for each of the layers used for specific solar cells. Hence, all these considerations have to be taken into account in order to assess the real significance of the numerical results. Even with these limitations, it will be shown that this kind of analysis is important and will help for a better understanding of the observed behavior for solar cells, as will be shown with the two examples below, where we have used AMPS-1D for making the simulations.

3.1. HIT Silicon solar cells

Sanyo Ltd. has developed a silicon solar cell called Hetero-junction with intrinsic thin layer (HIT) cell. The high-quality performance of these devices has been demonstrated by efficiencies over 22% in laboratory cells and over 20% in mass production cells based on textured n-type Czochralski (CZ) crystalline silicon (c-Si) (Taira et al., 2007; Tanaka et al., 2003).

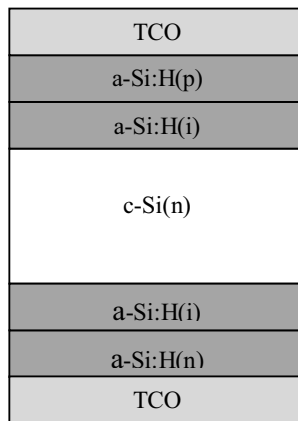


Fig. 1: Schematic diagram of the hetero-junction (HIT) amorphous/crystalline silicon structure with an intrinsic thin amorphous layer

In figure 1 (above), the schematics of the cell structure is shown. Notice that, in addition to the well known properties of crystalline silicon, the full parameters for both the extrinsic and intrinsic aSi layers is required. Fortunately this characterization has been done for aSi although the properties of the materials used in real solar cells usually are not reported, and we would have to assume that properties of pure layers grown at different laboratories than those where the cells are fabricated are the same for layer used in the solar cells, under similar deposition conditions.

We have used AMPS-1D for simulating this kind of solar cells. This simulation program has the limitation that no interface recombination is considered explicitly. However, by assuming a very thin layer with high (Shockley-Read-Hall) recombination it is possible to simulate a real interface. In figures 2-3 we show some of the results, when the parameters given in table 1 are assumed for the simulation (Hernandez-Como and Morales-Acevedo, 2010). We can notice the small total trap density (N_{ss}) at the interface between the intrinsic aSi and the crystalline silicon substrate required for achieving high efficiency HIT solar cells. In addition, we can observe the efficiency degradation for such solar cells when the interface density is increased above the required maximum N_{ss} value. Notice that the results show that N_{ss} above 10^{12} cm^{-2} will cause a strong degradation of the solar cell efficiency.

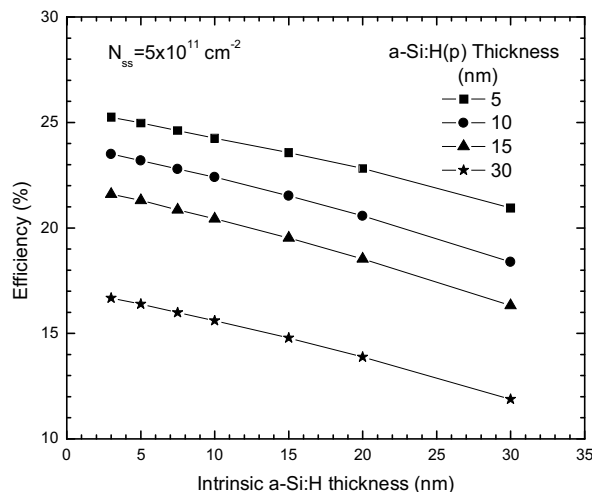


Fig. 2: Efficiency of the simulated HIT solar cells as a function of the intrinsic aSi layer thickness for different thickness of the p-type aSi emitter

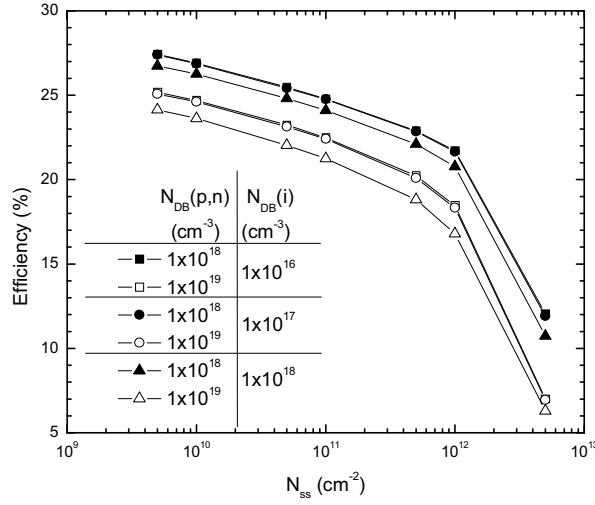


Fig. 3: Efficiency of the HIT solar cells as a function of the total density of states N_{ss} at the CSi/aSi(i) interface. Different Gaussian donor states are assumed in the p, n and intrinsic aSi layers.

Tab. 1: Parameter set for the simulation of hetero-junction solar cells with AMPS-1D

Parameter and units <i>e, h for electrons and holes respectively</i>	<i>a-Si:H(p+)</i>	<i>a-Si:H(i)</i>	<i>a-Si:H(n+)</i>	Layer at the <i>a-Si:H/c-Si</i> interface	<i>c-Si(n)</i>
Thickness (nm)	10	5	10	3	300000
Electron affinity (eV)	3.8	3.8	3.8	4.05	4.05
Band gap (eV)	1.72	1.72	1.72	1.12	1.12
Effective conduction band density (cm ⁻³)	2.50×10^{20}	2.50×10^{20}	2.50×10^{20}	2.80×10^{19}	2.80×10^{19}
Effective valence band density (cm ⁻³)	2.50×10^{20}	2.50×10^{20}	2.50×10^{20}	1.04×10^{19}	1.04×10^{19}
Electron mobility (cm ² V ⁻¹ s ⁻¹)	10	20	10	1350	1350
Hole mobility (cm ² V ⁻¹ s ⁻¹)	1	2	1	450	450
Doping concentration of acceptors (cm ⁻³)	3×10^{18}	0	0	0	0
Doping concentration of donors (cm ⁻³)	0	0	1×10^{19}	3×10^{15}	3×10^{15}
Band tail density of states (cm ⁻³ eV ⁻¹)	2×10^{21}	2×10^{21}	2×10^{21}	1×10^{14}	1×10^{14}
Characteristic energy (eV) donors, acceptors	0.06, 0.03	0.06, 0.03	0.06, 0.03	0.01	0.01
Capture cross section for donor states, e, h, (cm ²)	1×10^{-15} , 1×10^{-17}	1×10^{-15} , 1×10^{-17}	1×10^{-15} , 1×10^{-17}	1×10^{-15} , 1×10^{-17}	1×10^{-15} , 1×10^{-17}
Capture cross section for acceptor states, e, h, (cm ²)	1×10^{-17} , 1×10^{-15}	1×10^{-17} , 1×10^{-15}	1×10^{-17} , 1×10^{-15}	1×10^{-17} , 1×10^{-15}	1×10^{-17} , 1×10^{-15}
Total Gaussian density of states N_{DB} (cm ⁻³)	1×10^{18} – 5×10^{20}	1×10^{16} – 1×10^{18}	1×10^{18} – 5×10^{20}	0	0
Gaussian peak energy (eV) donors, acceptors	1.22, 0.70	1.22, 0.70	1.22, 0.70	0	0
Standard deviation (eV)	0.23	0.23	0.23	0	0
Capture cross section for donor states, e, h, (cm ²)	1×10^{-14} , 1×10^{-15}	1×10^{-14} , 1×10^{-15}	1×10^{-14} , 1×10^{-15}	0	0
Capture cross section for acceptor states, e, h, (cm ²)	1×10^{-15} , 1×10^{-14}	1×10^{-15} , 1×10^{-14}	1×10^{-15} , 1×10^{-14}	0	0
Total midgap density of states D_i (cm ⁻³ eV ⁻¹)	0	0	0	1×10^{16} – 1×10^{20}	1×10^{11}
Switch over energy (eV)	0	0	0	0.56	0.56
Capture cross section for donor states, e, h, (cm ²)	0	0	0	1×10^{-15} , 1×10^{-17}	1×10^{-15} , 1×10^{-17}
Capture cross section for acceptor states, e, h, (cm ²)	0	0	0	1×10^{-17} , 1×10^{-15}	1×10^{-17} , 1×10^{-15}

Another important result is related to the transparent conductor oxide properties, in particular its work function. In figure 4 we show the variation of efficiency as a function of the TCO work function. We can see that materials with a work function below 5 eV will cause efficiency degradation for this kind of solar cells. Then, we can see the importance of using ZnO(Al) instead of ITO for making better HIT solar cells. In other words, in this case it is not irrelevant the TCO used, as assumed by some experimentalist groups which have made HIT solar cells with a small work function TCO.

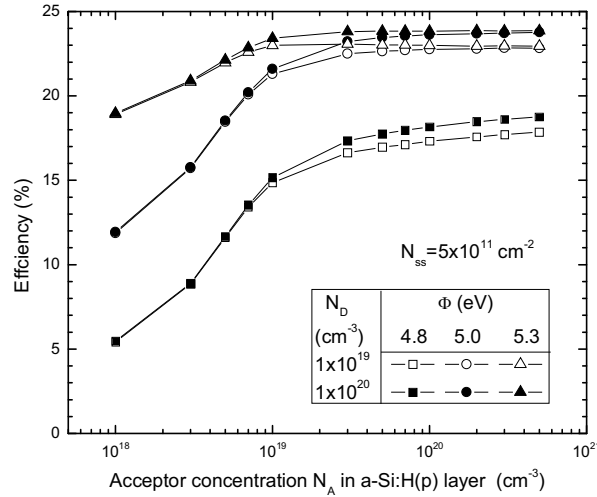


Fig. 4: Efficiency of the HIT solar cells as a function of the acceptor concentration in the p-type aSi layer for different TCO work functions

In summary, in the case of HIT solar cells where the parameters of aSi and cSi are relatively well known, numerical simulation allows establishing the required upper limit for the aSi-cSi interface trap density. It also reveals that a high work function TCO is required in order to have high efficiency. Of course, after a good numerical model has been achieved, the simulated solar cells can be optimized taking into account the technological limits for a specific laboratory.

3.2. CIGS solar cells

Contrary to the above example for silicon, solar cells based on thin film polycrystalline materials become more difficult to simulate numerically because most of the properties are not adequately known yet, and the poly-crystallinity character require a two or three dimensional solution of the transport equations. However, it has been established that recombination in the grain boundaries, which is the most important parameter affected by the presence of small crystallites, can be modeled by means of an “effective lifetime”. Carrier mobility can also be included in a solar cell model by assuming an “effective mobility”. And both of these parameters are related to an “effective diffusion length” (Morales-Acevedo, 2006), in such a way that a one dimensional model can be used for carrier transport in this kind of materials. Therefore, we have used this approach in order to model thin film polycrystalline solar cells.

In figure 5, we show the typical structure for a $\text{CuInGaSe}_2/\text{CdS}$ (CIGS) solar cell. One of the first problems encountered is that affinities (χ) for CIGS and CdS are reported with different values by different authors. Furthermore, the affinity of the crystalline materials is not necessarily the same for the same polycrystalline materials. Then, we always will have some uncertainty about the correct band diagram of the hetero-junction, unless the real band offsets are measured.

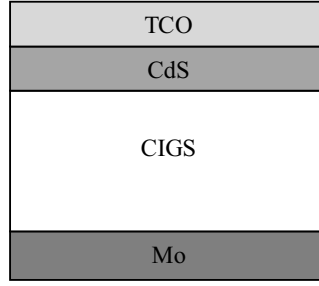


Fig. 5: Schematic diagram of the simulated hetero-junction CdS/CIGS solar cells

Notice that in CIGS solar cells, the band-gap of the material can be modified as a function of the $x = \text{Ga}/(\text{In}+\text{Ga})$ ratio in the film. It has been established that as a function of this ratio (x) the band-gap can be determined by:

$$E_g(x) = (1-x)E_g(\text{CIS}) + xE_g(\text{CGS}) - bx(1-x) \quad (\text{eq. 1})$$

where $E_g(\text{CIS}) = 1 \text{ eV}$, the band-gap for CuInSe_2 and $E_g(\text{CGS}) = 1.7 \text{ eV}$ is the band-gap for CuGaSe_2 . The “bowing” parameter has been determined to be approximately $b = 0.24$ (Wei et al., 1998).

Most of this band-gap variation is due to the modification of the electron affinity. Then, we have also a variation of the affinity as a function of x :

$$\chi(\text{CIGS}) = \chi(\text{CIS}) - [E_g(\text{CIGS}) - E_g(\text{CIS})] \quad (\text{eq. 2})$$

where $\chi(\text{CIS})$ is the electron affinity for CuInSe_2 .

In order to have a complete model we have taken into account the presence of two acceptor levels in CIGS. Schroeder et al. (1998) have measured the acceptor concentration and position within the band-gap so that the majority carrier concentration can be determined as a function of x .

Finally, since it is difficult to have absorption coefficients for the whole range of x , we have modeled the absorption coefficient by assuming a direct band material in all cases:

$$\alpha(h\nu, x) = \begin{cases} A\sqrt{h\nu - E_g(x)} & h\nu \geq E_g(x) \\ 0 & h\nu < E_g(x) \end{cases} \quad (\text{eq. 3})$$

Keeping the above uncertainties in mind, we modeled CIGS solar cells with the parameters defined in table 2. The purpose was to see if it is possible to obtain a reasonable simulation which could be compared with experimental results and other simulation calculations.

Tab. 2: Parameter set for CdS and CuInGaSe₂ for the simulation of CIGS solar cells

Parameter	CdS	CIGS
ϵ_s	10	13.6
μ_e (cm ² /V s)	10	50
μ_h (cm ² /V s)	5	25
N_A (cm ⁻³)	0	$\sim 1 \times 10^{16} - 1 \times 10^{19}$
N_D (cm ⁻³)	$1 \times 10^{16} - 1 \times 10^{17}$	0
E_g (eV)	2.42	1.00 – 1.68
N_C (cm ⁻³)	1.00×10^{19}	1.00×10^{19}
N_V (cm ⁻³)	1.00×10^{19}	1.00×10^{19}
χ (eV)	4.5	4.80 – 4.10
t_e (s)	-	1×10^{-8}
t_h (s)	1×10^{-9}	-
Thickness (nm)	100	3000

The first calculation (using AMPS-1D) was done by varying the carrier concentration in the CdS layer as a function of x (Ga content) for two different CdS layers. The result for the efficiency is shown in figure 6. We notice that only in the case of high carrier concentration (10^{17} cm^{-3}) in the CdS layer we can observe a monotonous growth of the efficiency for values of x up to 0.7. In the case of low carrier concentration (less than 10^{16} cm^{-3}), the efficiency is strongly reduced for $x < 0.5$ due to the presence of a spike in the CdS/CIGS interface affecting the filling factor of the cell.

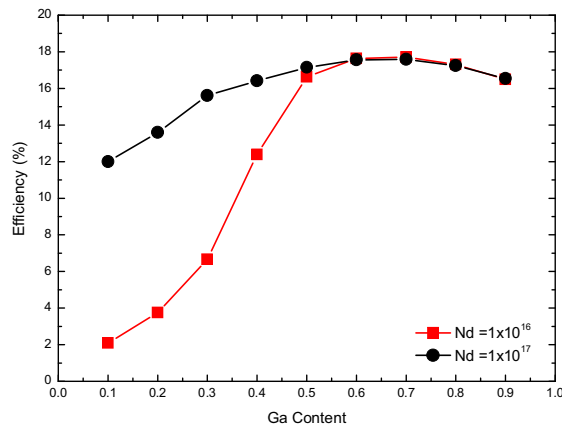


Fig. 6: Efficiency of the simulated CIGS solar cell as a function of Ga content in the CIGS layer. Two donor concentrations were assumed for the CdS layer

Notice that the optimum value of $x = 0.7$ corresponds to band-gap values of the CIGS layer around 1.45 eV. This value is in agreement to old calculation for the optimum band-gap in a solar cell. However, it is well established experimentally that the optimum efficiency for CIGS solar cells occurs for CIGS band-gap values between 1.15-1.2 eV. In order to explain this, it has been suggested that a very thin inversion layer (n-type layer) appears at the CIGS/CdS interface as a consequence of the processes for making the solar cell.

Therefore, we have included such (inversion) layer with the properties summarized in table 3 (above). In this case, we have used the high carrier concentration (10^{17} cm^{-3}) CdS layer. The result is shown in figure 7. Notice that in this case the optimum occurs for $x = 0.4$ which corresponds to a band-gap value of 1.22 eV which is more in agreement with the experimental result for the optimum band-gap. These results are also in agreement with those by other authors, but it seems to us that none of the previous works have obtained simulation results which allow the prediction of the high record conversion efficiencies reported for CIGS solar cells (above 20%).

Tab. 3: Physical parameters for modeling the inverted (CIGS) layer at the CdS and CIGS interface

Parameter	Inverted Surface Layer
ϵ_s	13.60
μ_e (cm ² /V s)	10
μ_h (cm ² /V s)	5
N_A (cm ⁻³)	0
N_D (cm ⁻³)	1×10^{15}
E_g (eV)	1.30
N_C (cm ⁻³)	1.00×10^{19}
N_V (cm ⁻³)	1.00×10^{19}
χ (eV)	4.5
t_h (s)	1×10^{-8}
t_e (s)	-
Thickness (nm)	30

According to the above discussion, we need further investigation in order to explain the disparity between the calculated maximum efficiency and the reported experimental record efficiency. It has been suggested that band-gap grading (Morales-Acevedo, 2009, 2010) can be a part of this, but in any case, a better understanding of the behavior of CIGS solar cells is still needed in order to foresee new ways to improve the efficiency of this kind of solar cells.

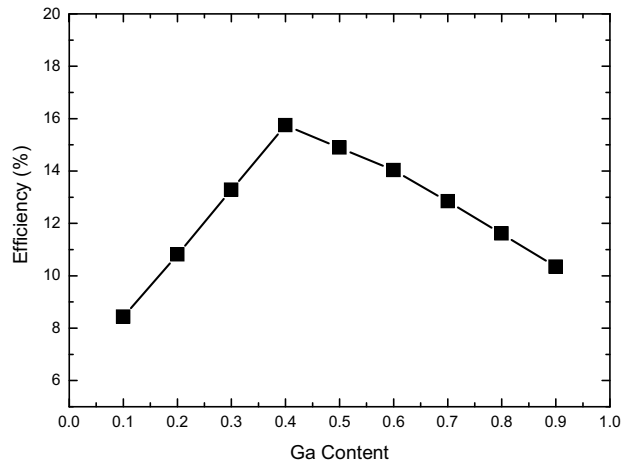


Fig. 7: Efficiency of the simulated CIGS solar cell where an inversion (n-type CIGS) layer was included at the CdS/CIGS interface. In this case the CdS layer donor concentration was assumed to be 10^{17} cm^{-3}

4. Conclusions

It has been shown that numerical simulation, preceded by simple analytical models, is an important tool for understanding and achieving high efficiency solar cells. Particularly, for materials for which most of the transport parameters are well known. Silicon, both in crystalline and amorphous phase, is one of those materials. In this case, the numerical calculations provide not only a good understanding but they also allow us to predict ways to improve the efficiency, for example of HIT solar cells. On the other hand, cells made from polycrystalline materials are more complex and the transport properties are not well known. In this case, numerical simulation helps for understanding the solar cell behavior, for example for CIGS/CdS solar cells it was shown that the inclusion of a CIGS (n-type) inverted layer between the CdS and the CIGS films gives a possible explanation for the observed optimum Ga content in the CIGS, although it does not explain the high record efficiencies observed experimentally. These results also suggest further characterizations to be made for CIGS layers and complete solar cells. For example, a better characterization of the band offsets at the CIGS and CdS interface, effective lifetimes and mobilities of minority carriers, in addition to the presence of the inverted layer is still needed. Other effects, such as the band-gap grading is also an effect to be investigated further which also can be modeled numerically.

5. Acknowledgements

This work was partially supported by CONACyT project No. 83042 and ICyTDF project ICyTDF/26/2010 . The authors would also like to thank Professor S. Fonash of the Pennsylvania State University for providing the AMPS-1D program used in the simulations.

6. References

- Basore P., 1990. Numerical modeling of textured silicon solar cells using PC-1D. *IEEE Transactions on Electron Devices*. 37(2), 337.
- Burgelman M., Nollet P., Degraeve S., 2000. Modeling polycrystalline semiconductor solar cells. *Thin Solid Films* 361-362, 527-532.
- Clugston D., Basore P., 1997. PC1D Version 5: 32-bit Solar Cell Modeling on Personal Computers. Conference Record of the 26th IEEE Photovoltaic Specialists Conference, Anaheim CA. 207-210.
- Froitzheim A, Stangl R, Elstner L, Kriegel M, Fuhs W., 2003. AFORS-HET a computer program for the simulation of heterojunction solar cells to be distributed for public use. Presented at the 3rd World Conference on Photovoltaic Energy Conversion, Osaka.
- Gray J. L., 1991. ADEPT: a general purpose device simulator for modeling solar cells in one- two and three dimensions. Conference Record of the 22nd IEEE Photovoltaic Specialists Conference, Las Vegas NV, 436-438.
- Hernandez-Como N., Morales-Acevedo A., 2010. Simulation of hetero-junction silicon solar cells with AMPS-1D. *Solar Energy Materials & Solar Cells*. 94, 62-67.
- Hurkx G. M., Klaassen D. B. M., Knuvers M. P. G., 1992. A new recombination model for device simulation including tunneling. *IEEE Transactions on Electron Devices* 39(2), 331-338.
- Morales-Acevedo A., 2006. Physical Basis for the Design of CdS/CdTe thin film Solar Cells. *Solar Energy Materials and Solar Cells* 90, 678-685.
- Morales-Acevedo A., 2009. Variable band-gap semiconductors as the basis of new solar cells. *Solar Energy* 83, 1466-1471.
- Morales-Acevedo A., 2010. A Simple Model of Graded Band-Gap CuInGaSe₂ Solar Cells. *Energy Procedia* 2, 169-176.
- Pauwels H., Vanhoutte G., 1978. The influence of interface states and energy barriers on the efficiency of heterojunction solar cells. *Journal of Physics D: Applied Physics* 11, 649-667.
- Schroeder, D.J., Hernandez, J.L., Berry, G.D. and Rockett, A.A., 1998. Hole transport and doping states in epitaxial CuIn_{1-x}Ga_xSe₂. *J. Appl. Phys.* 83 (3), 1519-1526.
- Smole F., Topic M., Furlan J., 1994. Amorphous silicon solar cell computer model incorporating the effects of TCO/a-Si:C:H junction. *Solar Energy Materials and Solar Cells* 34, 385.
- Taira S., Yoshimine Y., Baba T., Taguchi M., Kanno H., Kinoshita T., Sakata H., Maruyama E., Tanaka M., 2007. Our approaches for achieving HIT solar cells with more than 23% efficiency. *Proceedings of the 22nd European Photovoltaic Solar Energy Conference, Milan, Italy*. 932-935.
- Tanaka M., Okamoto S., Tsuge S., Kiyama S., 2003. Development of HIT solar cells with more than 21% conversion efficiency and commercialization of highest performance HIT modules. *Proceedings of the Third World Conference on Photovoltaic Energy Conversion, Osaka*. 955-958.
- Wei, S-H., Zhang, S.B., Zunger, A., 1998. Effects of Ga addition to CuInSe₂ on its electronic, structural and defect properties. *Appl. Phys. Lett.* 72, 3199-3201.